

# Reliability-based Multi-Objective Optimization and Visualization using LS-OPT<sup>®</sup> Version 4

Nielen Stander<sup>1</sup>, Willem Roux<sup>1</sup>, Tushar Goel<sup>1</sup>,  
David Björkevik<sup>2</sup>, Katharina Witowski<sup>3</sup>, Christoffer Belestam<sup>2</sup>

<sup>1</sup>Livermore Software Technology Corporation, Livermore, CA, USA 94551

<sup>2</sup>Engineering Research AB, Linköping, Sweden

<sup>3</sup>DYNAmore GmbH, Stuttgart, Germany

## Summary:

This study expounds the multi-objective optimization of a realistic crashworthiness problem with special reference to the incorporation of uncertainty and the visualization of the Pareto Optimal Frontier (POF). LS-OPT<sup>®</sup> and LS-DYNA<sup>®</sup> are used for the optimization based on the C2500 truck model developed by NHTSA. The design problem is set up as a Reliability-Based Design Optimization (RBDO) problem which includes specifications for the variation of the input parameters. For the purpose of design, reliability-based constraints on the displacements and stage pulses (interval-based integrals over the acceleration history) are specified. Nine thickness variables were assigned to various parts affecting the crashworthiness performance. Solution of the example employs Radial Basis Function networks as surrogate functions with Space Filling sampling as well as the NSGA-II algorithm for determining the POF starting from an infeasible design. Post-processing is done to determine a subset of optimal points of interest using the Viewer of LS-OPT<sup>®</sup> Version 4. This post-processor is based on a new architecture which allows window splitting and detachable windows for flexible viewing. It also includes the following new features: (1) Correlation Matrix, (2) Parallel Coordinate plot (POF) and (3) Hyper-Radial Visualization (POF). Thus 3 types of POF viewing are available, including the current 3D scatter plot. The study shows that a complex decision-making process such as optimal design involving uncertainty and multiple objectives can be simplified by using appropriate analysis and visualization tools.

## Keywords:

RBDO, Reliability-based Design Optimization, Crashworthiness optimization, Multi-Objective Optimization, LS-OPT

## 1 Introduction

Design technology has progressed significantly over the last decade so that today it is unusual to make engineering decisions based on a single physics simulation. Multiple analyses can be executed systematically by varying the design and using the combined results for design improvement. LS-OPT<sup>®</sup> [1] which has now been under development for more than a decade provides an environment for design and is tightly interfaced to LS-DYNA<sup>®</sup> [2] and LS-PREPOST<sup>®</sup> with the goal of allowing the user to organize input for multiple simulations and gather and display the results and statistics. More specifically, LS-OPT has capabilities for improving design performance in an uncertain environment and conducting system and material identification. These objectives can be achieved through the use of statistical tools, optimization and visualization.

Version 4 of LS-OPT features a new generation graphical postprocessor Viewer. The Viewer is based on a redesigned architecture that provides a much more flexible environment for the design engineer. The major enhancements are as follows:

- New plot types such as Correlation Matrix, Parallel coordinate plot, Hyper-radial Visualization (HRV).
- A higher level of interactivity in the various plots. E.g. the Correlation Matrix plot allows selection to enlarge the scatter plots or histograms for closer inspection while the Parallel Coordinate plot allows bounding of the functions in order to isolate a desirable design set.
- A split-window feature which allows multiple windows to be displayed in the same frame.
- Multiple ways of adding windows: replacing, splitting. Windows are detachable.
- Multiple simulation or predicted points can be selected and displayed in a spreadsheet format.
- The export and printing features have been significantly improved with the availability of most popular file formats.
- Integrated point selection, e.g. selected points are highlighted across multiple plot types.
- Zooming, which is useful for plots with high point density.

Other major features available in Version 4 is:

- a Post-processor capability which features the META post-processor [3] (Beta CAE Systems) for result extraction and
- the *LS-OPT<sup>®</sup>/Topology* optimization module featuring a linear/non-linear topology optimization capability integrated with LS-DYNA [4].

The current study employs a full vehicle finite element model to demonstrate the use of LS-OPT for multi-objective crashworthiness design in a probabilistic setting. The capabilities for visualizing the Pareto Optimal Frontier are demonstrated using this example.

## 2 Theoretical background

The purpose of multi-objective design is to compute an optimal hyper-surface representing the optimal designs for the case which has more than one design objective. Design conflicts between performance quantities are common in practical designs, e.g. Mass vs. durability in aerospace design or deceleration vs. mass vs. intrusion in automotive design. The multi-objective optimization capability in LS-OPT has been available since Version 3 when the NSGA-II [5] algorithm was implemented. The algorithm consists of a genetic algorithm which minimizes the objectives for a design population while maximizing the diversity of the population. This process eventually leads to points spanning the so called Pareto Optimal Frontier (POF). In general, the POF is a disjoint surface usually displayed in the objective function space as in Figure 2-1 (Feasible Objective Space). The optimization procedure yields the POF represented by a number of points (a non-dominated set). This set of points is represented by the thick red line in Figure 2-1. Since the designer is interested in the design variables associated with these designs, design exploration of the Pareto set is necessary to find suitable designs. This means that explorative tools are crucial to finding suitable designs. For this purpose, LS-OPT provides 3 features with a fourth under development. The three current features are:

1. *4-Dimensional scatter plot*: This is the most conventional tool with the fourth dimension represented by color. It works well for low dimensionality, i.e. with problems having only 2 or 3 objectives.
2. *Parallel Coordinate plot* [6]: This tool allows the plotting of all the objectives and variables on parallel axes with the point represented by the lines connecting all the axes. It works well for a small number of points since larger numbers of points tend to congest the display so that the lines are no longer distinguishable. To explore the design space, interactive tools are available to move the bounds on any function or variable in order to isolate a desirable set of optimal points. A typical usage is to bound the interesting points in the function space in order to obtain a set of desirable designs.
3. *Hyper-Radial Visualization* [7,8]: This methodology maps any number of objectives to a 2-dimensional space by allocating them to two groups and computing the distance in these group-based subspaces with respect to the Utopian design. The Utopian design is a hypothetical design (represented only in the objective space) obtained by minimizing each objective in isolation. A point in the 2D space is represented by these two distances. The advantage of the methodology is that the optimal points can be moved in the 2D space by adjusting the importance (represented by a weight) of each of the objectives. Thus the "best" point(s), i.e. the point(s) closest to the Utopian point can be obtained for any set of weights and used for the design.

*Integrated display*: LS-OPT integrates the above three methods by allowing the simultaneous display of all three while highlighting the user-selected points on all three plots. This feature is illustrated by the crashworthiness example presented in the next section.

An additional method, namely Self-Organizing Maps is also under development. That development is discussed in Reference [9].

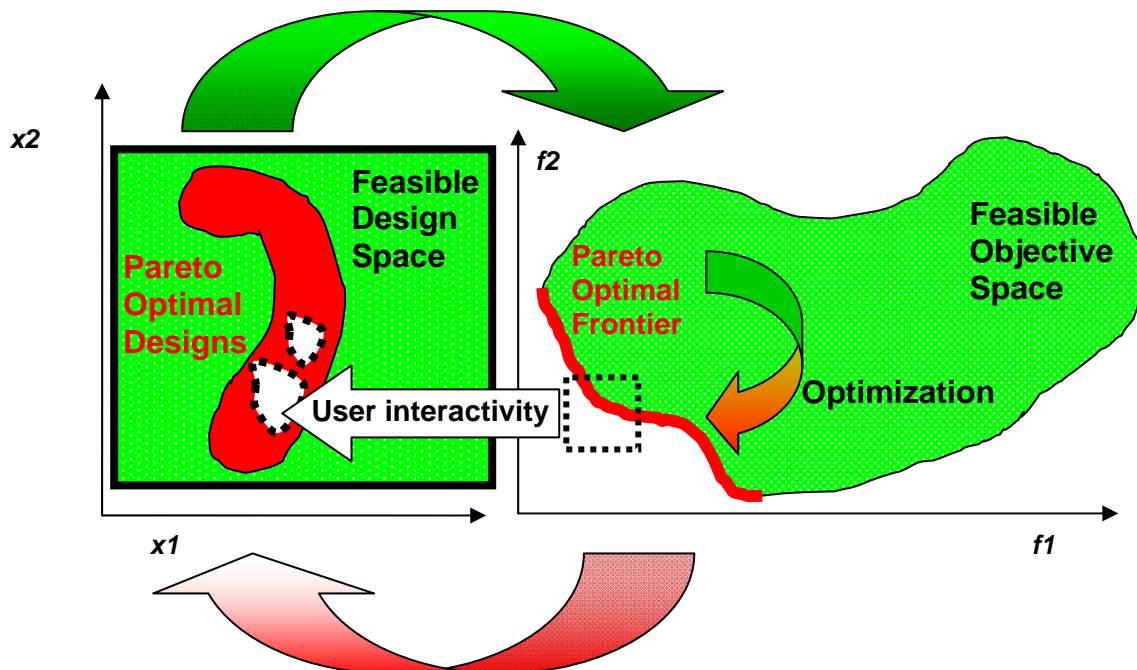


Figure 2-1: **Pareto Optimality**: Schematic diagram of the spaces of the independent design variables and dependent objective functions. The upper green arrow represents function evaluations at all the feasible points in the design space to create the feasible objective space (e.g. using metamodels of the design). The green-red arrow in the FOS represents the multi-objective optimization procedure (e.g. using NSGA-II). The lower red arrow represents the representation (through interactive visualization) of the Pareto Optimal Frontier to the design space for practical use in design. The straight white arrow (user interactivity) represents the selection of a desirable subset of Pareto Optimal points in the objective space.

The example is also used to illustrate the capabilities of the new Viewer features.

### 3 Example: Truck crashworthiness optimization

The example is a crashworthiness optimization problem that involves simulation of a National Highway Transportation and Safety Association (NHTSA) vehicle undergoing a full frontal impact. The finite element model for the full vehicle (obtained from NCAC website [10]), shown in Figure 3-1, has approximately 55K elements. Nine gauge thicknesses affecting the members listed in Table 1, are taken as design variables and affected parts are shown in Figure 3-1. Uncertainty of the exact thicknesses is quantified using a statistical distribution of the thickness (see Table 1).

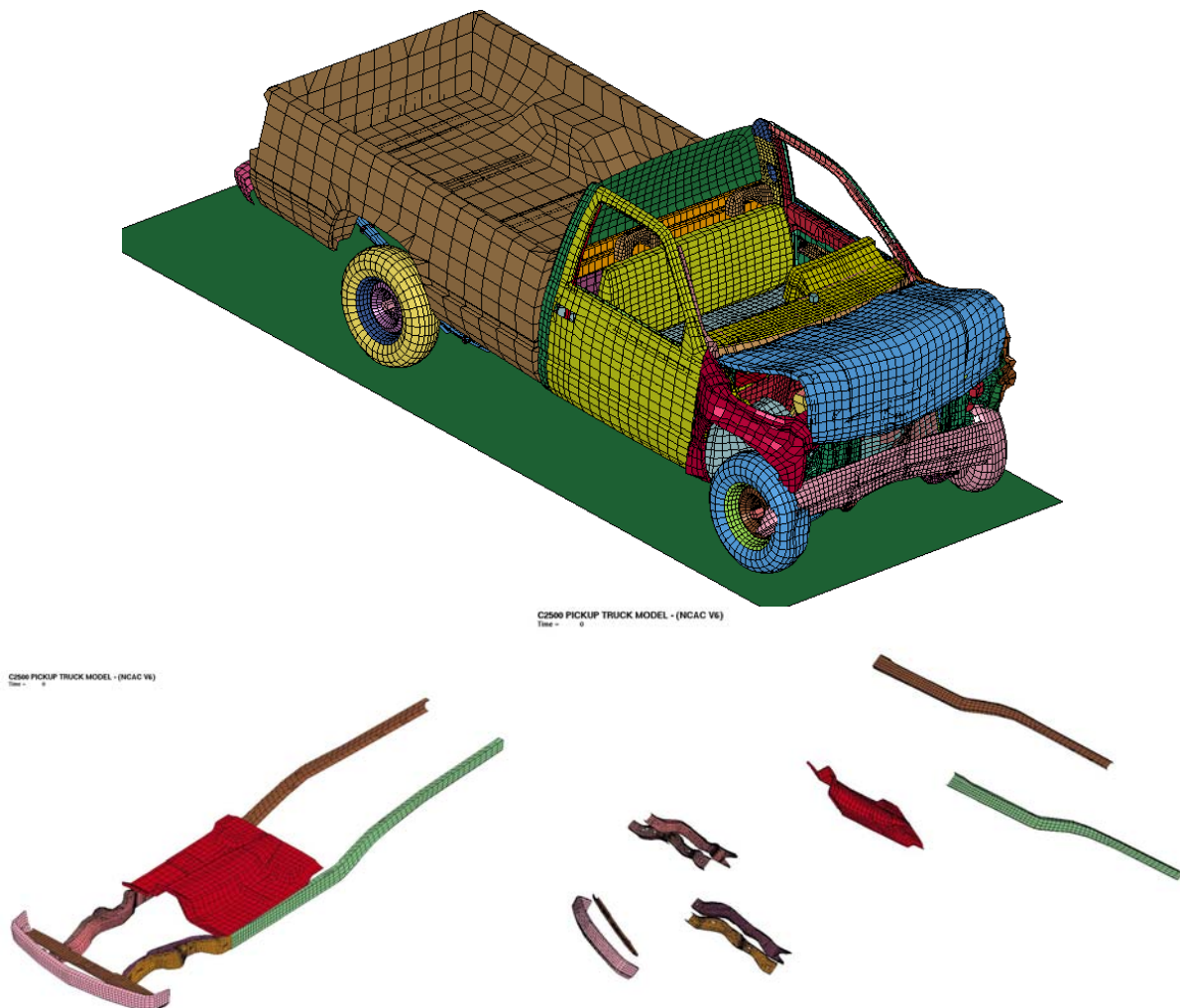


Figure 3-1: Finite element model, and thickness design variables for crashworthiness example.

The crash performance of the vehicle is characterized by considering the maximum acceleration, maximum displacement that links to intrusion, time taken by the vehicle to reach zero velocity state, and different stage pulses. These responses are taken at the accelerometer mounted in the middle of the front seat. To reduce the influence of numerical noise, SAE filtered acceleration (filter frequency 60Hz) is used and different entities are averaged over two accelerometer nodes. While constraints are imposed on some of these crash performance criteria (stage pulses), it is desirable to optimize the performance with respect to other criteria.

Table 1: Design variables for crash example

Variable description	Name	Lower bound	Baseline design	Upper bound	Distribution
Rail front-right-inner	t1	2.500	3.137	3.765	Uniform
Rail front-right-outer	t2	2.480	3.112	3.750	Uniform
Rail front-left-inner	t3	2.400	2.997	3.600	Uniform
Rail front-left-outer	t4	2.400	3.072	3.600	Uniform
Rail right-back	t5	2.720	3.400	4.080	Uniform
Rail left-back	t6	2.850	3.561	4.270	Trunc. Normal
Bumper	t10	2.160	2.700	3.240	Trunc. Normal
Radiator bottom	t64	1.000	1.262	1.510	Trunc. Normal
Cabin bottom	t73	1.600	1.990	2.400	Trunc. Normal

Thus a multi-objective optimization problem can be formulated as follows:

*Minimize:*

Mass and peak acceleration;

*Maximize:*

Time-to-zero-velocity and maximum displacement;

subject to constraints on variables and performance.

Table 2: Design constraints

	Upper bound	Probability of exceeding the upper bound
Maximum displacement ( $x_{crash}$ )	721 mm	0.15
Stage 1 pulse (SP1)	7.48 g	0.15
Stage 2 pulse (SP2)	20.20 g	0.15
Stage 3 pulse (SP3)	24.50 g	0.15

The design variable bounds and input distribution are given in Table 1 and the performance constraints, namely maximum displacements and stage pulses, are specified in Table 2. The three stage pulses are calculated from the averaged SAE filtered (60Hz) acceleration  $\ddot{x}$  and displacement  $x$  of the accelerometer nodes in the following fashion:

$$-\frac{k}{(d_2 - d_1)} \int_{d_1}^{d_2} \ddot{x} dx \quad k = 0.5 \text{ for } j = 1, k = 1.0 \text{ otherwise}; \quad (3)$$

The integration limits  $(d_1; d_2) = (0; 200); (200; 400); (400; \text{Max}(x_{crash}))$  for  $j = 1, 2, 3$  respectively, represent different structural crash events. All displacement units are *mm* and the minus sign is used to convert acceleration to deceleration. During optimization, all objectives and constraints are scaled to avoid dimensionality issues.

The LS-DYNA<sup>®</sup> [2] explicit solver was used to simulate the crash. Each crashworthiness simulation takes approximately 5 hours using one core of a fully loaded quadcore Intel Xeon 5365 processor and generates an output of 225 MB. A 640-core HP XC cluster, comprising 80 ProLiant server nodes of two Intel Xeon 5365 quad-core processors (also known as Clovertown, with 2 processors/8 cores), with a 3.0 GHz clock rate, was used to run the required 1000 simulations. More details about running the simulation appear in Reference [5].

## 4 Input specification

The input data is prepared in the LS-OPT GUI by specifying the solver data (input files, executables, queuing interface) as well as the variable data (starting values, bounds and distribution) (Figure 4-1). The desired responses available from the LS-DYNA database are selected in the Histories and

Responses pages of the GUI. The constraints and objectives are also defined in the respective GUI pages (Figure 4-2). Note that all the objectives are maximized, and that the Mass and acceleration quantities are pre-multiplied by -1 because of the requirement to minimize them. The four constraints are defined in terms of their probability of failure on the upper bound, namely 0.15.

In the Sampling page (not shown here) the Radial Basis Function networks are chosen as metamodels with 1000 Space Filling simulation points. These are presently the fastest and most accurate surrogate models available in LS-OPT. The points are all run in a Single Stage as selected on the Strategy page (2<sup>nd</sup> main tab) which means that they will all be created as part of a single large run instead of sequentially. A sequential run can also be scheduled for which similar results can be expected (see e.g. Reference [11]).

The screenshot shows the LS-OPT GUI with the 'Variables' tab selected. The main window displays a table of design variables. Three smaller windows are overlaid, showing the configuration for Uniform and Truncated Normal distributions, including mean and standard deviation values.

Type	Name	Starting	Init. Range	Minimum	Maximum	Distribution
Variable	t1	3.137		2.5	3.765	Uniform
Variable	t2	3.112		2.48	3.75	Uniform
Variable	t3	2.997		2.4	3.6	Uniform
Variable	t4	3.072		2.4	3.6	Uniform
Variable	t5	3.4		2.72	4.08	Uniform
Variable	t6	3.561		2.85	4.27	Truncatec
Variable	t10	2.7		2.16	3.24	Truncatec
Variable	t64	1.262		1	1.51	Truncatec
Variable	t73	1.99		1.6	2.4	Truncatec

Figure 4-1: Definition of design variables with upper and lower bounds as well as noise properties of the uniform and truncated normal distributions.

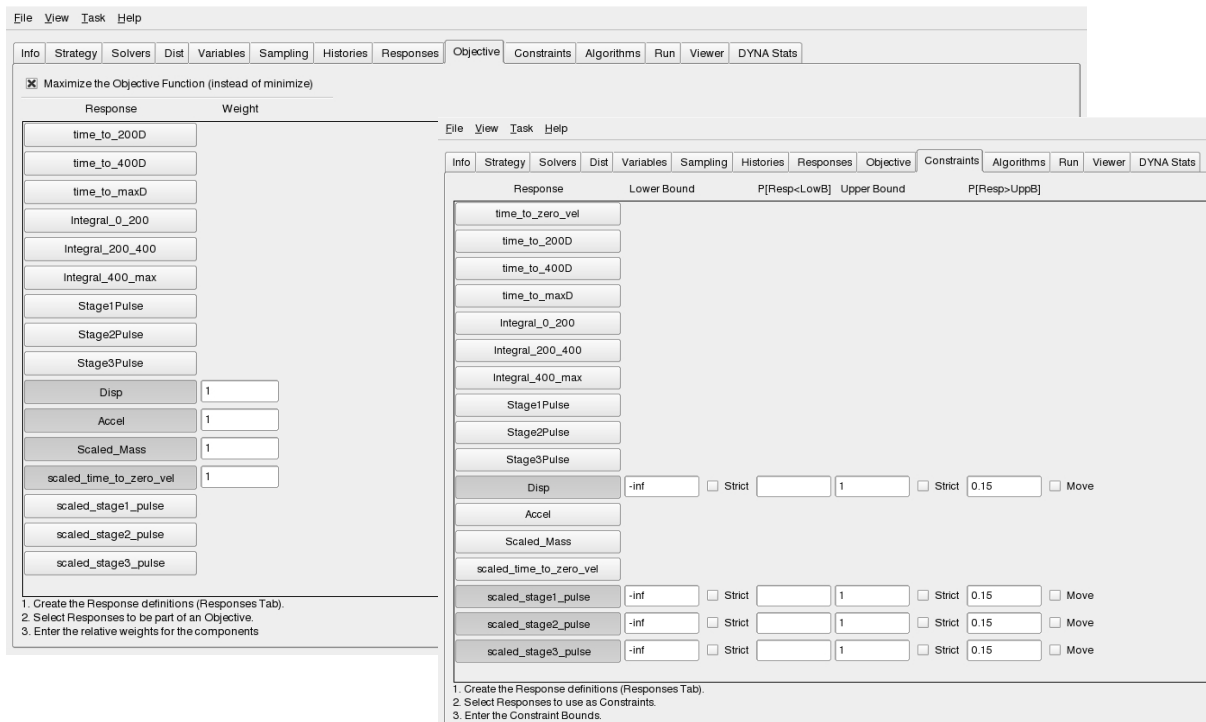


Figure 4-2: Definition of Objectives and Constraints.

## 5 Results and observations

Figure 5-1 displays the correlation matrix of the 1000 simulation points. To be noted in the upper triangle is the low cross-correlation of the input variables as well as some negative (shades of blue) or positive (shades of red) correlations with respect to the performance variables. The lower triangle displays the corresponding scatter plots while the diagonal displays the distribution of the input variables and responses obtained from the simulations.

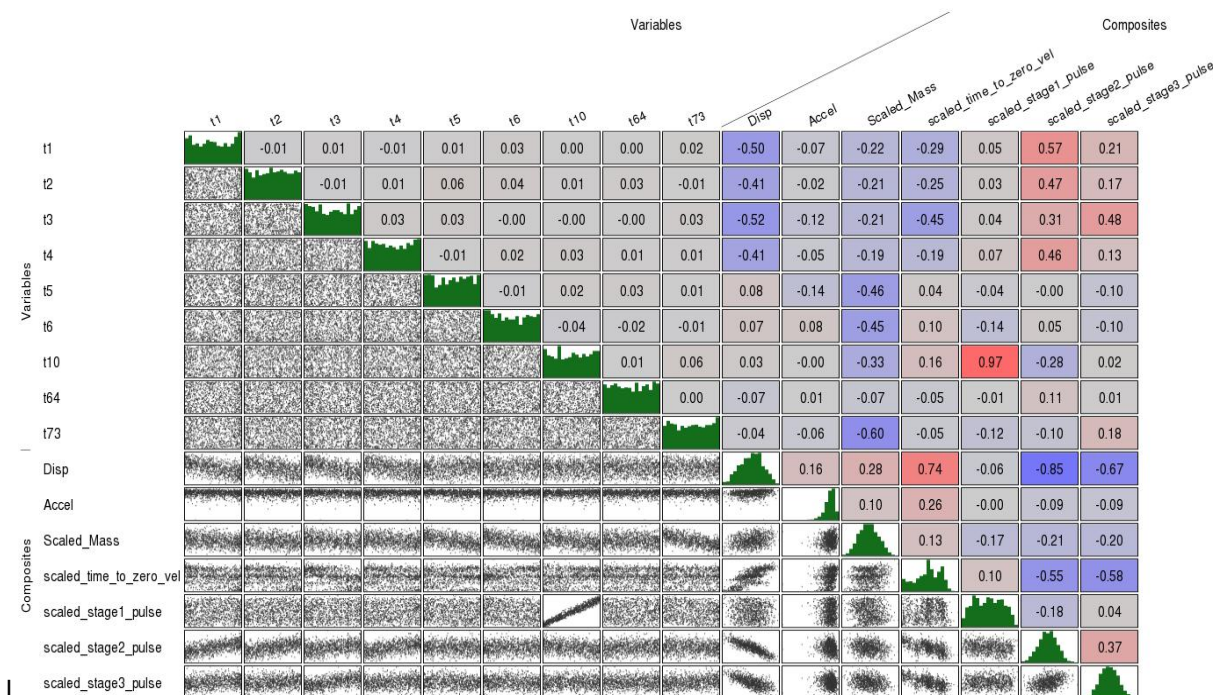


Figure 5-1: Correlation plot of simulation points



Figure 5-2 represents the accuracy of the RBF metamodelling (in this case composite functions of the basic responses) as depicted by Predicted vs. Computed plots. Error measure information about the basic responses (e.g. RMS error, PRESS error and  $R^2$  error) can be found in the accuracy plots for responses or report files (not shown here). The points in the Accuracy plot are color coded (red/green) according to feasibility. Note the extremely small degree of feasibility of the design space: only five points out of approximately 1000 are feasible.

The initial feasibility status of the response in terms of the output distribution and probability of failure can be found in Figure 5-3. Note that the starting design is infeasible, i.e. three of the four constraints are violated since the probabilities of failure of these three constraints exceed the upper bound of 0.15 being 1, 1 and 0.745 for the Stage 1, 2 and 3 pulses respectively.

Figure 5-4 displays the stochastic contribution of each of the design variables to each of the selected performance variables (responses). The stochastic contribution represents the contribution of the noise (in terms of the standard deviation of the noise distribution) of each of the variables to the total response variation. Note how for instance  $t_{10}$  has a very significant contribution to the Stage 1 Pulse and  $t_3$  has a significant contribution to the Stage 3 Pulse.

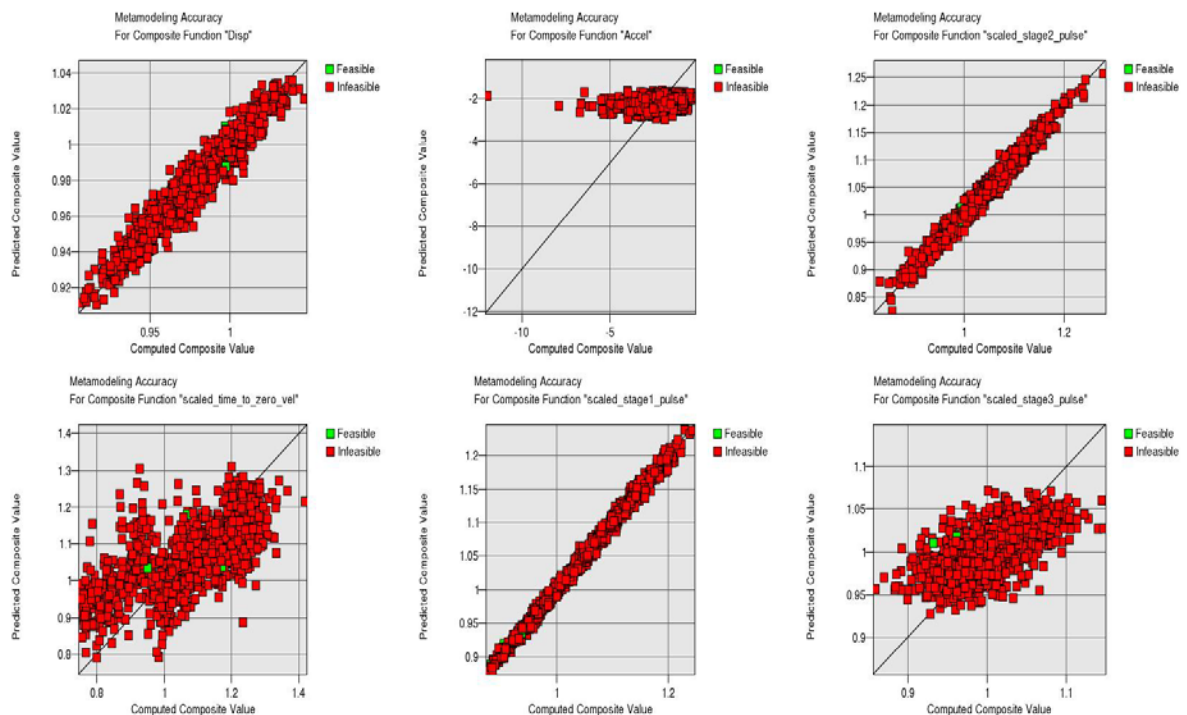


Figure 5-2: Metamodel accuracy



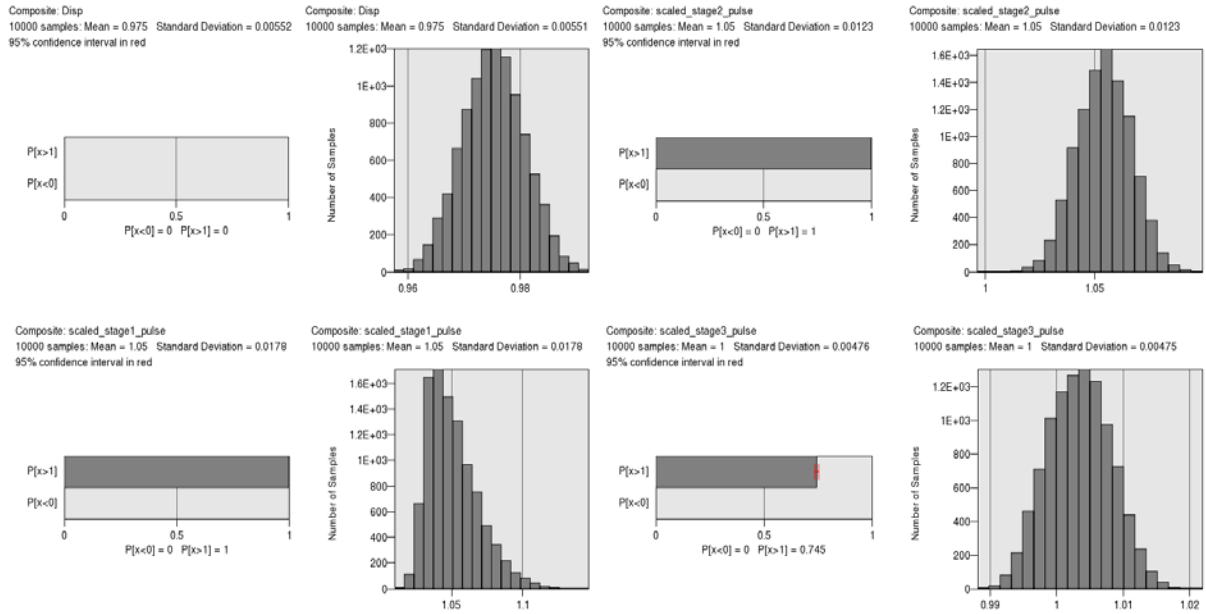


Figure 5-3: Distribution of the constraint functions at the initial design point (baseline design). The probability of failure is represented by the horizontal bar charts. Note that only the upper bound value is bounded at 0.15 probability of failure.

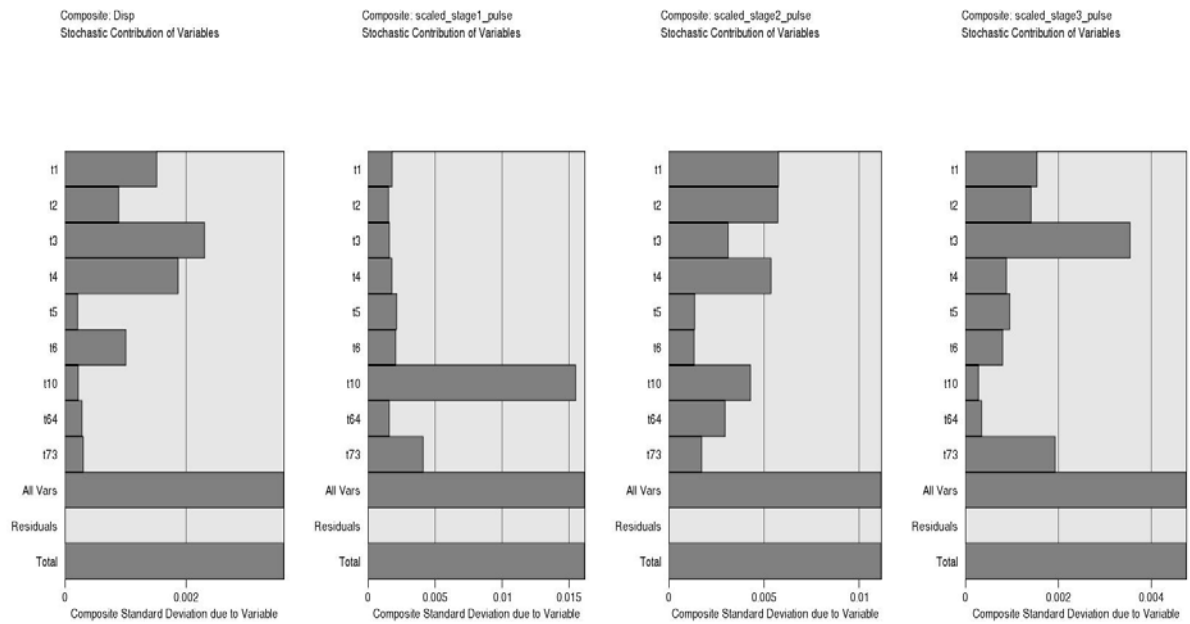


Figure 5-4: The stochastic contribution of the variables to the output variation (baseline design).

The optimization procedure using NSGA-II yields an often large set of non-dominated points which is reduced to an evenly distributed smaller set of 100 for greater clarity of visualization. Figure 5-5 displays this subset of the original Pareto Optimal set determined by the GA algorithm. Three different plots are shown namely (i) a three-dimensional scatter plot (top left), (ii) Hyper-Radial Visualization (top right) and (iii) the Parallel Coordinate plot (bottom). A thickness value of  $t_5$  as a function of each point is depicted in color on the upper plots. The parallel coordinate plot was used to select and print a smaller subset of optimal points (a second level of reduction, see Figure 5-6). The smaller set was

obtained by bounding the objective functions as shown in Figure 5-5. The points in the HRV diagram are the result of equal weighting of the objective functions. The user can also adjust the weights for finding interesting points for different scenario's of objective weights.

Figure 5-7 depicts the optimization history of the four objective functions for a single Pareto optimal point namely the one with equal weights of all the objective functions (not shown here). The final point shown in Figure 5-7, obtained through equal weighting of the objectives, was chosen as an optimum to analyze further in terms of the feasibility of the different constraints. Figure 5-8 depicts the final estimates of the constraint distributions. Note that the design is now feasible, i.e. the probability of failure  $< 0.15$  with the Disp constraint the critical one. The Stage 1 Pulse also plays a significant role while the other stage pulses have almost zero probability of failure.

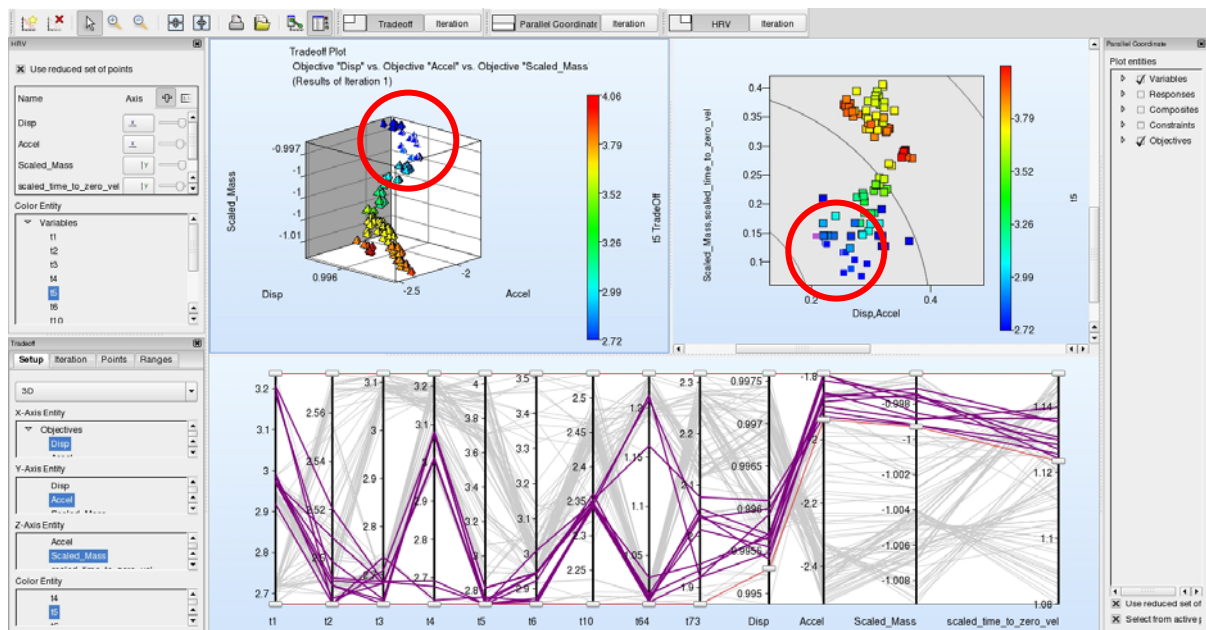


Figure 5-5: Interface showing Reduced Pareto Set using three different plot types: Three-dimensional scatter plot (top left), Hyper-Radial Visualization (top right) and Parallel Coordinate plot (bottom) of a few points selected by the user in the Parallel Coordinate plot. The grey lines in the Parallel Coordinate plot represent points excluded by the interactive bounding of the constraints using the sliders (the 4 values on the extreme right of the PC plot are maximized as far as possible). The statistics of the 8 selected points are displayed in the spreadsheet shown in Figure 5-6. Note cross-highlighting of selected points (circled in red). The point closest to the Utopian point is also highlighted in purple on the HRV diagram.

Point selection		Variables												
Point	ID	t1	t2	t3	t4	t5	t6	t10	t64	t73	N1_disp	N2_disp	N1_a	
t1.61														
t1.62														
t1.71														
t1.76	t1.61	2.97461	2.48845	2.63813	3.0794	2.81527	2.94545	2.34648	1.00323	2.03686	717.13	718.566	138	
t1.80	t1.314	2.97028	2.60838	2.68088	3.01328	2.73141	2.94295	2.34327	1.01036	1.93423	717.33	718.472	135	
t1.83	t1.339	2.97033	2.48855	2.6456	3.07694	2.72019	2.86593	2.34345	1.00244	1.92001	717.046	718.437	135	
t1.99	t1.360	2.97461	2.49834	2.64825	3.08183	2.81396	2.94505	2.35213	1.20886	2.0356	718.167	718.057	140	
t1.113	t1.381	2.98462	2.4904	2.68054	3.00673	2.72048	3.00838	2.34825	1.01035	2.04238	716.999	718.375	135	
t1.128	t1.388	3.2071	2.52048	2.68494	2.6768	2.72071	2.92279	2.36076	1.00453	2.05429	717.589	718.2	132	
t1.144	t1.395	3.18645	2.49159	2.68559	2.69227	2.72118	2.86564	2.34113	1.00694	2.01281	717.287	718.296	132	
t1.151														
t1.156	t1.510	3.20129	2.48092	2.73607	2.64129	2.76148	2.86426	2.3466	1.02748	1.94592	717.561	718.189	133	
t1.161														
t1.172														

Figure 5-6: Spread sheet format of Pareto Optimal points selected interactively (Figure 5-5).

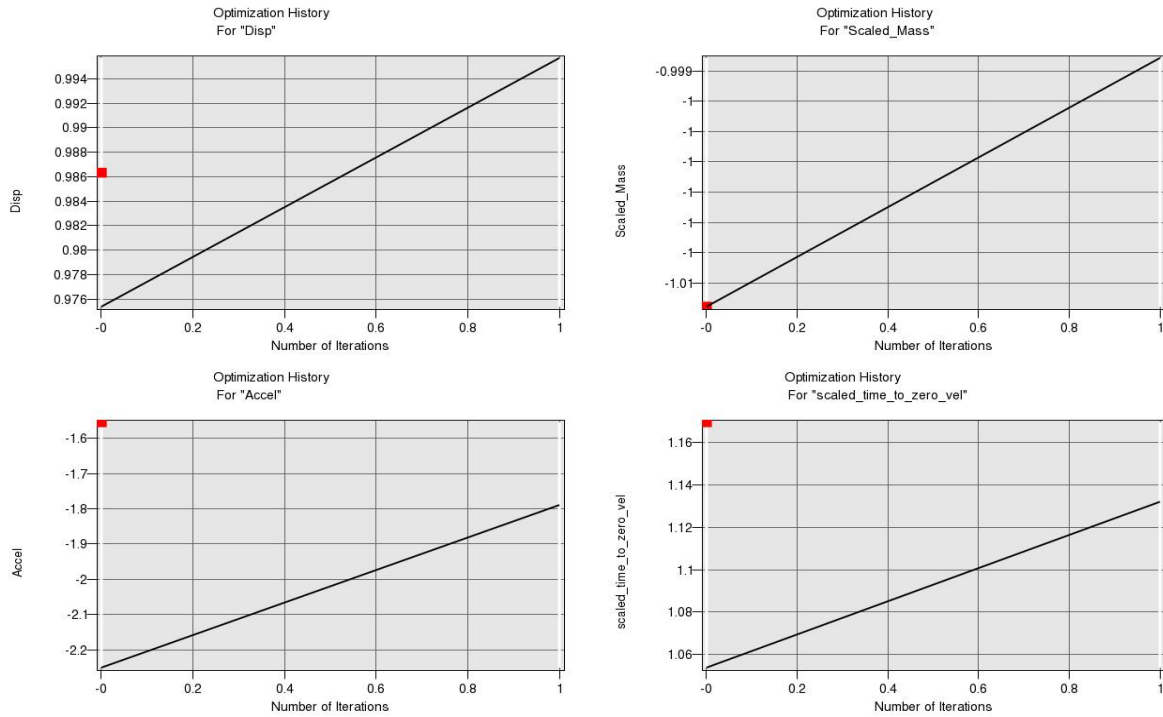


Figure 5-7: Optimization history of maximization problem of the equally weighted design (one of the Pareto Optimal designs). The baseline design results are shown as red points.

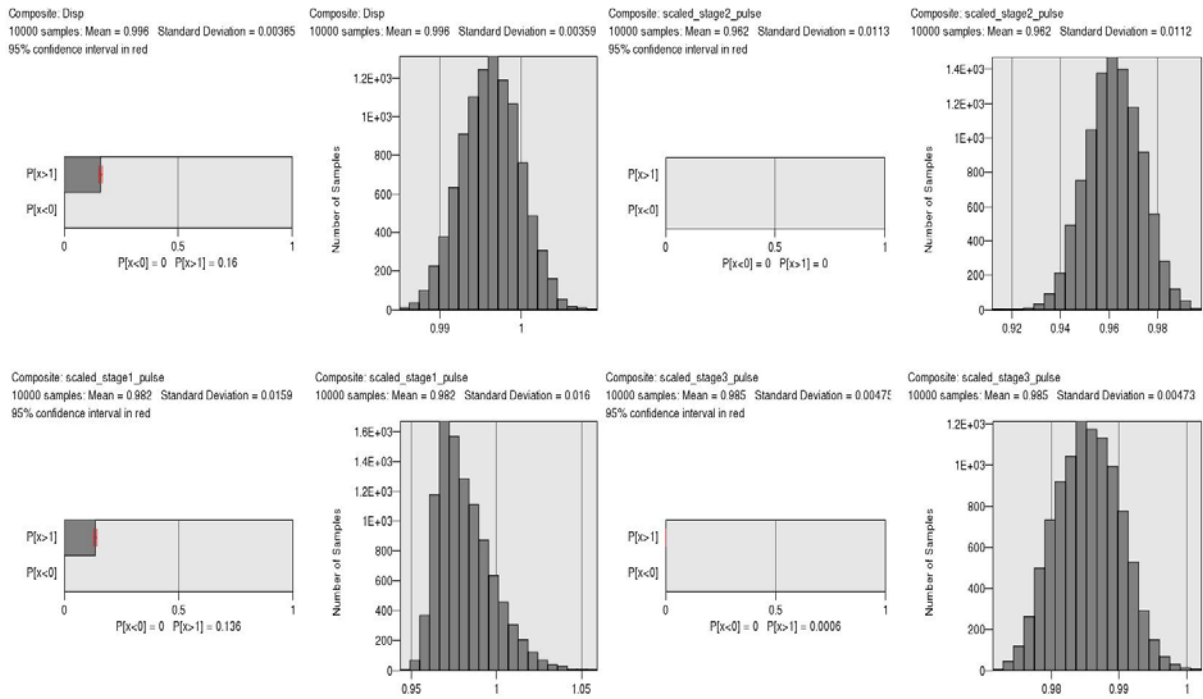


Figure 5-8: Distribution of the constraint functions at an optimal design point, the equally weighted design from Figure 5-7. The probability of failure is represented by the horizontal bar charts. Note that only the upper value is bounded at 0.15 probability of failure. Only the Disp, an intrusion constraint is active (top left).

## 6 Conclusions

This study briefly describes the solution of a multi-objective reliability-based design optimization problem using LS-OPT. It is shown that Version 4 provides a significantly enhanced Viewer for flexible visualization and reporting of optimization results. New features to visualize the Pareto Optimal Front have been added. The new architecture provides greater flexibility for further development and refinement of the LS-OPT visualization features.

## 7 Literature

- [1] Stander, N., Roux, W.J., Goel, T., Eggleston, T., Craig, K.-J. *LS-OPT<sup>®</sup> User's Manual, Version 4*, Livermore Software Technology Corporation, Livermore, California, USA, April, 2009.
- [2] J.O. Hallquist, *LS-DYNA<sup>®</sup> Version 971 User's Manual*, Livermore Software Technology Corporation, October 2007.
- [3] Korbetis, G., Siskos, D. Multi-disciplinary design optimization exploiting efficiency of ANSA-LSOPT-META coupling, Proceedings of the 7<sup>th</sup> European LS-DYNA Conference, Salzburg, Austria, May 14-15, 2009.
- [4] Goel, T., Roux, W.J., Stander, N. Topology Optimization using LS-DYNA. Proceedings of the 7<sup>th</sup> European LS-DYNA Conference, Salzburg, Austria, May 14-15, 2009.
- [5] Goel, T., Yih-Yih Lin, Stander, N. Direct Multi-Objective Optimization through LS-OPT using a small number of crashworthiness simulations. Proceedings of the 10<sup>th</sup> International LS-DYNA Users Conference, Detroit, Michigan, U.S.A., May, 2008.
- [6] d'Ocagne, Maurice. *Coordonnées Parallèles et Axiales: Méthode de transformation géométrique et procédé nouveau de calcul graphique déduits de la considération des coordonnées parallèles*. Paris: Gauthier-Villars, 1885.
- [7] Chiu, P.-W. and Bloebaum, C.L. Hyper-Radial Visualization (HRV) for Decision-making in Multi-Objective Optimization. Proceedings of the 46<sup>th</sup> AIAA Aerospace Sciences Meeting and Exhibit, 7-10 January 2008, Reno, Nevada.
- [8] Chiu, P.-W. and Bloebaum, C.L. Hyper-Radial Visualization (HRV) with Weighted preferences for multi-objective decision making. Proceedings of the 12<sup>th</sup> AIAA/ISSMO Multidisciplinary Analysis and Optimization Conference, 10-12 September 2008, Victoria, British Columbia, Canada.
- [9] Witowski, K., Liebscher, M. and Goel, T. Decision making in Multi-Objective Optimization for Industrial Applications – Data mining and visualization of Pareto data. Proceedings of the 7<sup>th</sup> European LS-DYNA Conference, Salzburg, Austria, May 14-15, 2009.
- [10] National Highway Traffic Safety Administration. <http://www.nhtsa.dot.gov>.
- [11] Stander, N. and Goel, T. Metamodel sensitivity to sampling strategies: a crashworthiness design study, Proceedings of the 10<sup>th</sup> International LS-DYNA Users Conference, Detroit, Michigan, U.S.A., May, 2008.